A New Synchronous Rectification for Phase Shift Modulation LLC Resonant Converter

Koji Murata*‡, Fujio Kurokawa**

*Dep. of Electrical and Electronics Engineering, Nagasaki University, Nagasaki, Japan

** Dep. of Electrical and Electronics Engineering, Faculty of Engineering, Nagasaki University, Nagasaki, Japan

(ijok64@gmail.com, fkurokaw@nagasaki-u.ac.jp)

‡Corresponding Author; Koji Murata, Dep. of Electrical and Electronic Engineering, Nagasaki University, Nagasaki, 852-8137, Japan, Tel: +81 95 819 2489, Fax: +81 95 819 2488, ijok64@gmail.com

Received: 31.10.2015 Accepted:15.11.2015

Abstract- This paper presents a new synchronous rectification (SR) for phase shift modulation (PSM) LLC resonant converters. The SR for PSM LLC resonant converter has difficulty because the secondary current is not in phase with both primary current and the voltage across the transformer. Furthermore, the open-loop SR for phase shift modulation does not perform well because the optimum pulse width is highly dependent on operating conditions such as the duty ratio of primary switches and the load current condition. The proposed SR utilizes the average load current to predict the optimum pulse width of SR so that the detection circuit for SR is not required. Effectiveness of the proposed SR is simulated and experimentally verified.

Keywords LLC resonant converter; phase shift modulation; synchronous rectification; full-bridge; predict.

1. Introduction

Many studies on LLC resonant converters have been done so far because it has advantages over the conventional resonant converters. From many advantages such as soft-switching capability, LLC resonant converter has been used as front-end converter [1, 2].

In recent years, LLC resonant converter for the renewable energy systems such as solar or battery charger has been studied [3-8]. The phase shift modulation (PSM) LLC resonant converters have been attracting attention [6-13]. The phase shift modulation function is applied in LLC resonant converter in [6-8]. To reduce the power consumption of phase shift modulation LLC resonant converter, the synchronous rectification (SR) is important. The SR for PSM resonant converter has difficulty due to the discontinuous conduction of secondary current. The optimum turn-off timing for SR differs from the turn-off timing of driving signals in the primary side. The optimum pulse width of driving signals for synchronous rectification (SR) is longer than the on-time of primary bridge circuit. When the pulse width for SR is optimized under the heavy load condition, the reverse current flows through under the light load conditions. When the pulse width for SR is optimized at the light load condition, the conduction loss increases in the parasitic diodes of SRs especially at a small duty ratio. The difference of the timing between the turn-off of primary switches and optimum turn-off of secondary switches depends on the operating conditions such as the duty ratio and load current.

The detection circuit for SR of LLC resonant converter increases the number of components and cost. The SR for PFM LLC resonant converter without detection circuit is proposed in [14, 15]. In [14], the constant pulse width for SR is used because the variation of optimum pulse width is small. With this simple method, the efficiency is dramatically improved from LLC resonant converter with diode rectifier. The SR based on the relationship $D*V_O$ = constant is proposed [15]. However, both methods cannot be applied to PSM LLC resonant converters.

This paper presents a new SR for phase shift modulation LLC resonant converter. In the proposed method, the optimum turn-off timing is predicted from the average of load current. The average of load current is sensed in various applications such as constant current mode of battery charger [16, 17] and phase shedding of interleaving [18]. In ref. [19], although load current is not sensed, the average of load current is calculated from the voltage across the resonant capaci-

tor, which is used for active load sharing [20, 21] and improvement of transient responses [22]. In the proposed SR, the current detection circuits for SRs are not required by utilizing the information of the average load current. Effectiveness of the proposed SR is simulated and experimentally verified.

2. Operation Principle

2.1. Phase Shift Modulation LLC Resonant Converter

Figure 1 shows the circuit configuration of full-bridge type LLC resonant converter. V_i is the input voltage. Switches S_1 through S_4 convert the dc voltage V_i into the ac voltage v_b. The voltage v_b is the input of LLC resonant circuit formed with resonant inductance L_r, magnetizing inductance L_m and resonant capacitance C_r. The switches S_5, S_6 and output smoothing capacitor C_o form the rectifier stage. i_r, i_m, i_o indicate the current flowing through primary side, magnetizing inductance and secondary side.

Figure 2 shows the operation principle of phase shift modulation (PSM) LLC resonant converters operating at the resonant frequency of L_r and C_r. v_{gs1} through v_{gs6} are the drive signals for switches S_1 through S_6, respectively. T_{on} indicates on-time of driving signals of primary switches. D_p is the ratio between the on-time T_{on} and the time that diagonal switches S_1, S_3 or S_2, S_4 are on, which is the duty ratio of primary full-bridge circuit. T_c is the conduction time of secondary current i_o. In the case of PSM LLC resonant converter, driving signals v_{gs1} and v_{gs2} are synchronized with v_{gs3} and v_{gs4}, respectively. With the phase shift modulation, the driving signals v_{gs3} and v_{gs4} are shifted from the driving signals S_1 and S_2. When the switch S_1 and S_4 or S_2 and S_3 are on simultaneously, the input voltage of resonant circuit becomes zero. During this period, the input source is disconnected from the second stage of LLC resonant circuit. Although the input source is disconnected from the resonant circuit stage, the power is transferred to the secondary side of transformer and the load. Therefore, even after the primary stage becomes off-state, the SR stage must keep on-state for a certain time. T_c is the ideal pulse width of driving signals for SR v_{gs5} and v_{gs6}.

2.2. Proposed Synchronous Rectification

The operation of PSM LLC resonant converter is classified into 3 states in order to derive the optimum pulse width of driving signals for SRs as shown in Fig. 3. During the state 1, input voltage is applied to the LLC resonant circuit. The resonant inductor resonates with resonant capacitor. The current during this state is expressed as Eq. (1).

a

$$i_o(t) = I_{peak} \sin(2\pi \cdot f_r \cdot t) \tag{1}$$

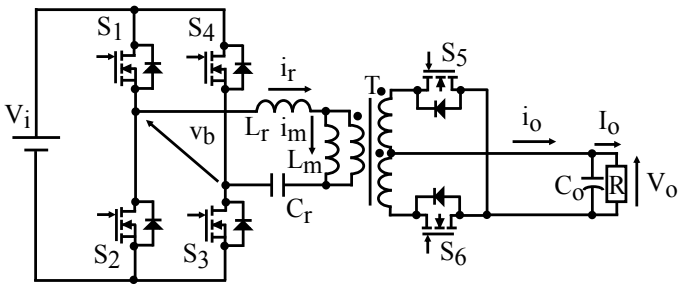

Fig. 1. Configuration of LLC resonant converter with synchronous rectification.

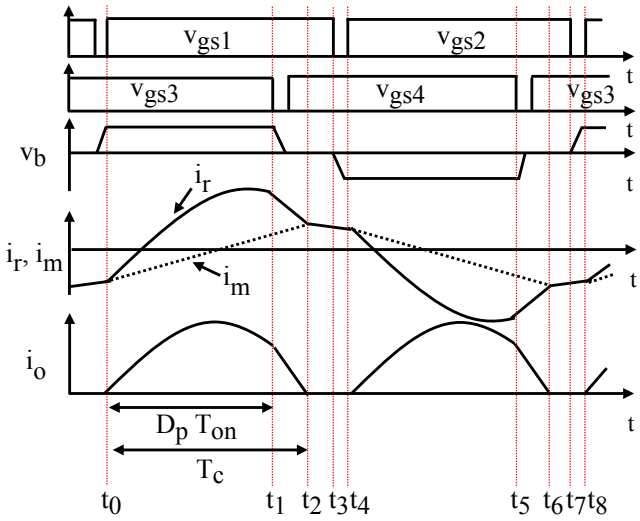

Fig. 2. Operation principle of PSM LLC resonant converter.

where

$$f_r = \frac{1}{2\pi\sqrt{L_r \cdot C_r}}$$

I_{peak} is the peak current of secondary current i_o.

During the state 2, the secondary current decreases linearly to zero. The secondary current i_o is the difference of the primary resonant current i_r and the magnetizing current i_m, which is expressed as Eq. (2).

$$i_o(t) = n \cdot \{i_r(t) - i_m(t)\} \tag{2}$$

where n denotes the number of turn ratio of transformer.

The primary current during this interval is expressed as Eq. (3).

$$i_r(t) = i_r(t_1) - \frac{V_L}{L_r} \cdot t \tag{3}$$

where $i_r(t_1)$ is the initial value of primary resonant current in the state 2 and V_L is the voltage across the resonant inductor during state 2.

The magnetizing current during this interval is expressed as Eq. (4).

$$i_m(t) = i_m(t_1) + \frac{n \cdot V_o}{L_m} \cdot t \tag{4}$$

where $i_M(t_1)$ is the initial value of the magnetizing current in state 2.

Thus, using Eqs. (2) through (4), the output current during this interval can be expressed as Eq. (5)

$$i_o(t) = i_o(t_1) - n\left(\frac{V_L}{L_r} + \frac{n \cdot V_o}{L_m}\right) \cdot t \tag{5}$$

At the end of this state, the secondary current becomes zero so that by calculating $i_O(t_2)$=0, the period of state 2 is derived as Eq. (6).

$$t_a = \frac{L_r \cdot L_m}{n \cdot (L_m \cdot V_L + L_r \cdot n \cdot V_o)} I_{peak} \cdot \sin(2 \cdot \pi \cdot f_r \cdot D_p \cdot \frac{T_s}{2}) \tag{6}$$

where

V_L is voltage across the resonant inductor.

During the state 3, the secondary current is zero, which is expressed as Eq. (7)

$$i_o(t) = 0 \tag{7}$$

The peak current I_{peak} and voltage across the resonant inductor are unknown parameters. The peak current I_{peak} is calculated from the average of load current as follows.

The average of load current is expressed as Eq. (8).

$$I_o = \frac{2}{T_s + 2 \cdot t_d} \int_0^{\frac{T_s + 2 \cdot t_d}{2}} i_o(t) dt \tag{8}$$

where

t_d is the dead time of driving signals of S_1, S_2 and S_3, S_4.

By using Eqs. (1), (5), (7) and (8), the peak of secondary current is derived as Eq. (9).

$$I_{peak} = \frac{-b + \sqrt{b^2 + 2 \cdot a \cdot I_o}}{a} \tag{9}$$

where

$$a = \frac{2}{T_s + 2 \cdot t_d} \frac{L_r \cdot L_m}{n \cdot L_m \cdot V_L + L_r \cdot n^2 \cdot V_o} \{\sin(\frac{T_s}{T_r} \cdot D_p \cdot \pi)\}^2$$

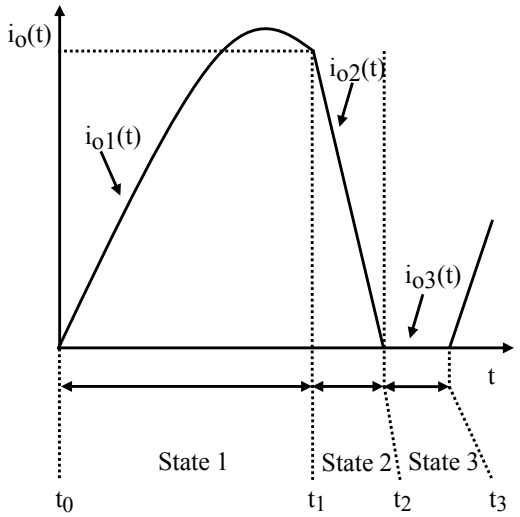

Fig. 3. Classification of operation states.

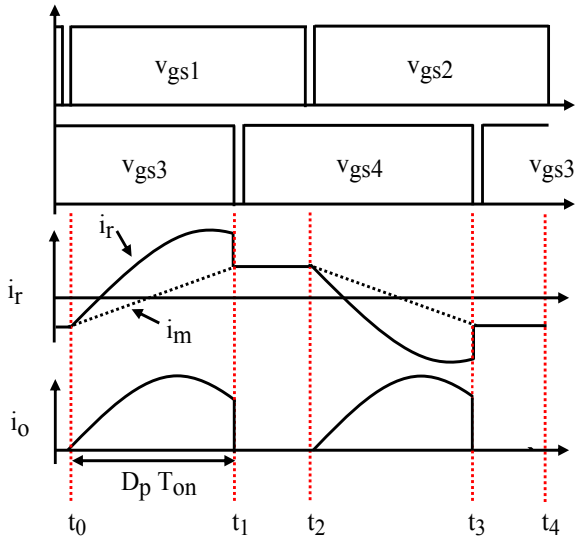

Fig. 4. Waveform with assumptions (1) and (2).

$$b = \frac{T_r}{T_s + 2 \cdot t_d} \frac{\{1 - \cos(\frac{T_s}{T_r} \cdot D_p \cdot \pi)\}}{\pi}$$

Next the unknown variable V_L is derived as follows. The voltage across the resonant inductor is expressed as Eq. (10).

$$V_L = V_{cr} + n \cdot V_o \tag{10}$$

To derive the equation of voltage V_L, the voltage across the resonant capacitor in state 2 V_{cr} is derived. To derive the expression of voltage across the resonant inductor in state 2, V_L, a few assumptions are made. The waveform with below assumptions is described in Fig. 4.

1) The slope of the decreased primary resonant current is infinite.

2) The magnetizing current during the off-time of primary full-bridge circuit is constant.

The voltage across the resonant capacitor in state2 V_{cr} which is the voltage at t_1 is expressed as Eq. (11).

$$V_{cr} = \frac{I_o}{4C_r n}(T_s + 2t_d) - \frac{D_p T_s}{4C_r}\frac{nV_o}{L_m}\frac{(1-D_p)\frac{T_s}{2}}{2} \quad (11)$$

The voltage in the state 2 can be expressed using Eqs. (10) and (11) as Eq. (12).

$$V_L = \frac{I_o}{4C_r n}(T_s + 2t_d) - \frac{D_p T_s}{4C_r}\frac{nV_o}{L_m}\frac{(1-D_p)\frac{T_s}{2}}{2} + nV_o \quad (12)$$

From above discussion, all unknown parameters for Eq. (6) are derived. The predicted pulse width for SR T_{ca} is expressed as Eq. (13).

$$T_{ca} = D_p \cdot T_{on} + t_a \quad (13)$$

Using Eq. (13), the proposed SR is performed.

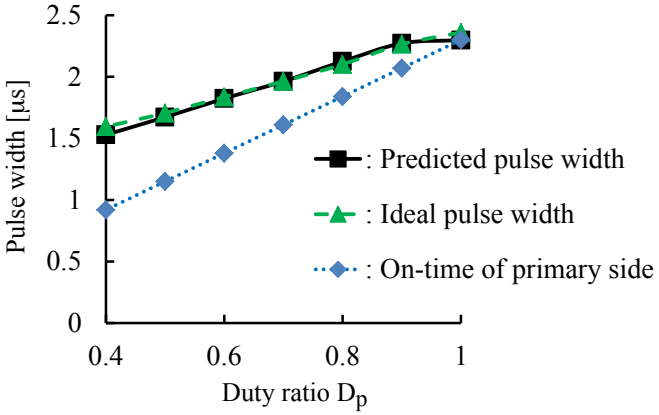

(a) I_O = 4 A

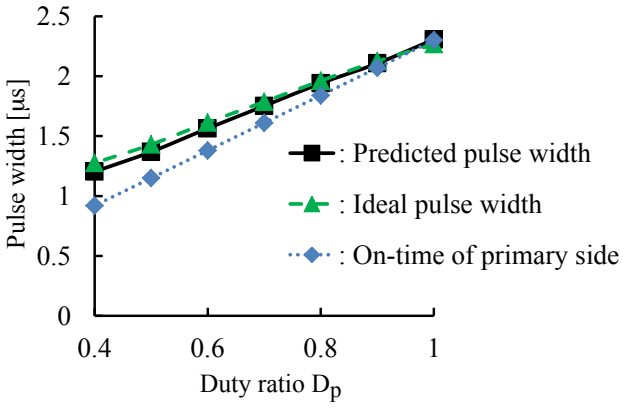

(b) I_O = 1 A

Fig. 5. Simulated comparison of ideal pulse width and predicted pulse width.

3. Simulated and Experimental Results

The parameter in the simulation and experiment are as follows. The resonant inductance L_r, magnetizing inductance L_m and the resonant capacitance C_r is 36 μH, 66 μH and 20 nF. The turn-ratio of transformer n is 9. The output voltage V_O = 5 V. The switching frequency f_S is 192 kHz. PSIM is used in the simulation. Figure 5 shows the simulated results of the predicted pulse width, ideal pulse width and the on-time of primary side. As it can be seen, there is a large difference between the on-time of primary side and the ideal pulse width.

As the duty ratio of primary full-bridge circuit D_p decreases, the ideal pulse width differs from on-time of primary side. Also, as the load gets heavier, the ideal pulse width for SR differs from the on-time of primary side. The simulated waveforms of proposed SR are shown in Fig, 6. Fig. 6(a) shows the waveform in the case of I_O = 4 A and D_p = 0.4. After the full bridge circuit in the primary side becomes off, the drive signals v_{gs5} and v_{gs6} is kept on until the secondary current decreases to almost zero. The waveforms of I_O = 1A is shown in Fig. 6(b). Figs. 7(a) and (b) show the corresponding experimental waveforms in the case of I_O = 4 A and 1A,

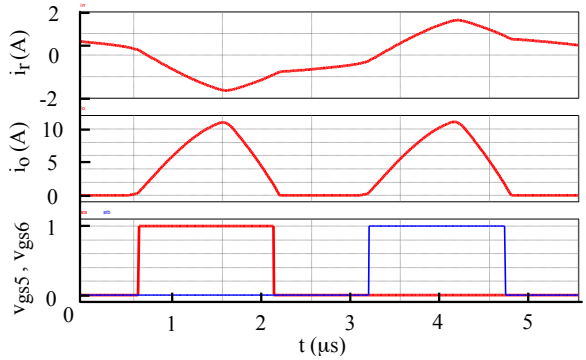

(a) I_O = 4 A

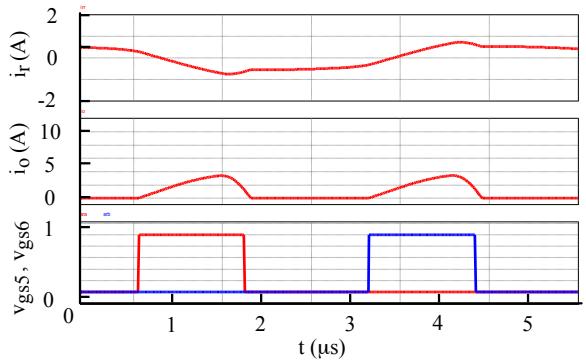

(b) I_O = 1 A

Fig. 6. Simulated results of proposed SR.

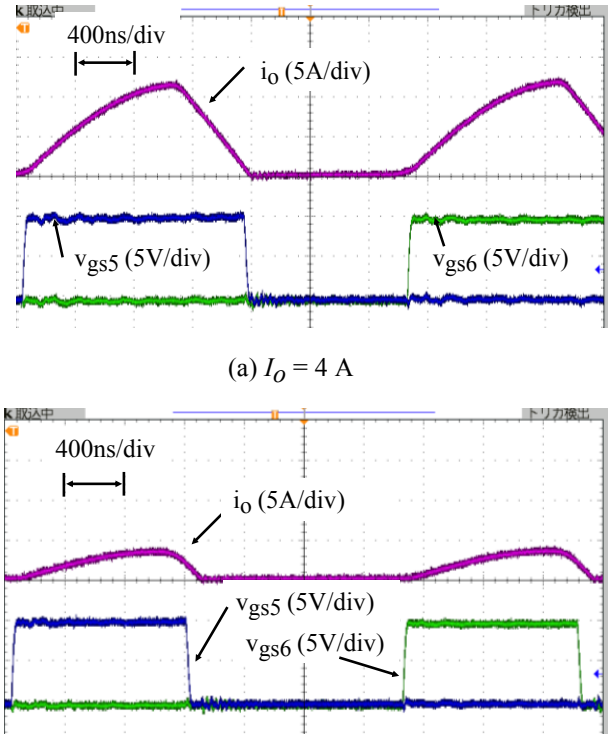

(a) I_O = 4 A

(b) I_O = 1 A

Fig. 7. Experimental results of proposed SR.

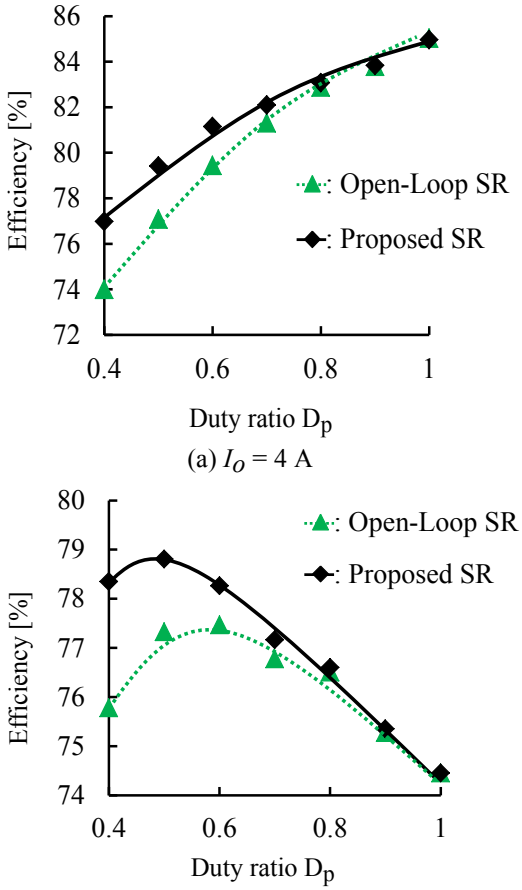

(a) I_O = 4 A

(b) I_O = 1 A

Fig. 8. Efficiency of PSM LLC resonant converter with SR.

respectively. The pulse width for SR is accurately predicted in both the simulation and experiment.

Figure 8(a) shows the experimental results of efficiency characteristics of PSM LLC resonant converter with the open-loop SR and proposed SR in the case of I_O = 4 A. The conduction loss caused by forward voltage drop of parasitic diodes of secondary switches is still significant. The proposed method can significantly improve the efficiency of PSM LLC resonant converter using the average value of load current. The efficiency of proposed SR is improved by 3% at duty ratio D_p = 0.4. Fig. 8(b) shows the experimental results of the efficiency of both SRs in the case of I_O = 1 A. The efficiency in the light load is also improved by proposed SR.

Conclusion

In this paper, a new synchronous rectification is proposed. The average of load current is utilized in the proposed SR. The secondary current is assumed pure sinusoidal waveform. The accuracy of the proposed method is investigated in the simulation. It is revealed that the proposed SR almost matches the ideal pulse width. The efficiency in the proposed SR is improved by 3% compared to the open-loop SR. The effectiveness of the proposed method is simulated and experimentally verified.

References

[1] B. Yang, F. C. Lee, A. J. Zhang and G. Huang, "LLC resonant converter for front end dc/dc conversion," Proc. of IEEE Applied Power Electronics Conference and Exposition, vol. 2, pp. 1108-1112, Mar. 2002.

[2] B. Lu, W. Liu, Y. Liang, F. C. Lee, J. D. van Wyk, "Optimal design methodology for LLC resonant converter," Proc. of IEEE Applied Power Electronics Conference and Exposition, pp. 533-538, Mar. 2006.

[3] J. Deng, S. Li, S. Hu, C. Chris Mi, and R. Ma, "Design methodology of LLC resonant converters for electric vehicle battery chargers," IEEE Trans. Vehicular Technology, vol. 63, no. 4, pp. 1581-1592, May 2014.

[4] F. Musavi, M. Craciun, D. S. Gautam, W. Eberle, and W. G. Dunford, "An LLC resonant dc–dc converter for wide output voltage range battery charging applications, "IEEE Trans. Power Electronics, vol. 28, no. 12, pp. 5437-5445, Dec. 2013.

[5] Y. S. Dow, H. I. Son, and Hyeoun-Dong Lee, "A study on half bridge LLC resonant converter for battery charger on board," Proc. of IEEE International Conference on Power Electronics and ECCE Asia, 2011, pp. 2694-2698.

[6] P. Deck and C. Peter Dick, "Improved modulation strategy for a LLC-type resonant converter in a solar application," Proc. of IEEE International Exhibition and Conference for Power Electronics, Intelligent Motion, Renewable Energy and Energy Management, pp.772-779, May 2014.

[7] C. P. Dick, P. Deck and A. Schmidt, "Optimized buck - mode modulation strategy and control of a LLC - type resonant converter in a solar application," Proc. of IEEE European Conference on Power Electronics and Applications, pp. 1-9, Aug. 2014.

[8] N. Shafiei, M. Ordonez, M. Cracium, M. Edington and C. Botting, "High power LLC battery charger: wide regulation using phase-shift for recovery mode," Proc. of IEEE Energy Conversion Congress and Exposition, pp. 2037-2042, Sep. 2014.

[9] B. McDonald and F. Wang, "LLC performance enhancements with frequency and phase shift modulation control," Proc. of IEEE Applied Power Electronics Conference and Exposition, pp. 2036-2040, Mar. 2014.

[10] J.-Hyun Kim, C.-Eun Kim, J.-Bum Lee, Y.-Do Kim, H.-Shin Youn and G.-Woo Moon, "A simple control scheme for improving light load efficiency in a full-bridge LLC resonant converter," Proc. of IEEE International Power Electronics Conference, pp. 1743-1747, May 2014.

[11] K. Murata and F. Kurokawa, "A novel interleaved LLC resonant converter with phase shift modulation," Proceedings of IEEE Energy Conversion Congress and Exposition, pp. 2051-2056, Sep. 2014.

[12] S. Liu, R. Ren, W. Meng, X. Zheng, F. Zhang, L. Xiao, "Short-circuit current control strategy for full-bridge LLC converter," Proc. of IEEE Energy Conversion Congress and Exposition, pp. 3496-3503, Sep. 2014.

[13] X. Li, H.-Yu Li and G.-Yuan Hu, "Modeling of a fixed-frequency resonant LLC dc/dc converter with capacitive output filter," Proc. of IEEE Energy Conversion Congress and Exposition, pp. 5456-5461, Sep. 2013.

[14] J. Wang and B. Lu, "Open loop synchronous rectifier driver for LLC resonant converter," Proc. of IEEE Applied Power Electronics Conference and Exposition, pp. 2048-2051, Mar. 2013.

[15] S. Abe, T. Zaitsu, J. Yamamoto and S. Ueda, "Adaptive driving of synchronous rectifier for LLC converter without signal sensing," Proc. of IEEE Applied Power Electronics Conference and Exposition, pp. 1370-1375, Mar. 2013.

[16] K. Colak, E. Asa, D. Czarkowski, "Dual Closed Loop Control of LLC Resonant Converter for EV Battery Charger," Proc. of IEEE International Conference on Renewable Energy Research and Applications, pp. 811-815, Oct. 2013.

[17] B.-Chul Kim, K.-Bum Park, C.-Eun Kim, B.-Hee Lee and G.-Woo Moon, "LLC resonant converter with adaptive link-voltage variation for a high-power-density adapter," IEEE Trans. on Power Electronics, vol. 25, no. 9, pp. 2248-2252, Sep. 2010.

[18] M. Kim, "Two-phase interleaved LLC resonant converter with phase shedding control," Proc. of IEEE International Power Electronics Conference, pp. 1642-1645, Jun. 2010.

[19] Z. Hu, Y.-Fei Liu, and P. C. Sen, "Cycle-by-cycle average input current sensing method for LLC resonant topologies," Proc. of IEEE Energy Conversion Congress and Exposition, pp. 167-174, Sep. 2013.

[20] Z. Hu, Y. Qiu, Y.-Fei Liu, and P. C. Sen, "An interleaving and load sharing method for multiphase LLC converters," Proc. of IEEE Applied Power Electronics Conference and Exposition, pp. 1421-1428, Mar. 2013.

[21] Z. Hu, Y. Qiu, L. Wang, and Y.-Fei Liu, "An interleaved LLC resonant converter operating at constant switching frequency," IEEE Trans. on Power Electronics, vol. 29, no. 6, pp. 2931-2943, Jun. 2014.

[22] Z. Hu, Y.-Fei Liu and P. C. Sen, "Bang–bang charge control for LLC resonant converters," IEEE Trans. on Power Electronics, vol. 30, no. 2, pp. 1093-1108, Feb. 2015.